Viscoelasticity Measurement of Heart Wall in *in vivo*

Hiroshi Kanai
Department of Electronic Engineering, Graduate School of Engineering, Tohoku University,
Sendai 980-8579, Japan. Email: hkanai@ecei.tohoku.ac.jp

***Abstract*— By measuring spatial distribution of the minute vibrations in the heart wall from the chest wall using ultrasound, we find that some impulses propagate along the heart wall in healthy human subjects just after closure of the aortic valve for the first time. Their amplitude is found to be on the order of several tens of micrometers, and up to 100 Hz. Their propagation speed shows frequency dispersion, which agrees with the theoretical characteristics of the Lamb wave. The instantaneous viscoelasticity of the wall is then noninvasively determined. These findings have a novel potential for myocardial tissue characterization in clinical diagnosis.**

I. Introduction

Magnetic resonant imaging [1], [2], computer tomography [3], and conventional ultrasonography enable clinical visualization of cross-sectional images of the human heart, but their imaging is restricted to large motion ($>$ 1 mm) and low frequency components ($<$ 30 Hz). Analysis of the motion-mode (M-mode) image [4], [5]—the magnitude of the sequentially obtained radio frequency (RF) data acquired in conventional echocardiography—is a candidate for transthoracic measurement of the heart-wall motion. However, the detectable amplitude is still greater than the wavelength, which is equal to 410 μm for ultrasound with a frequency of 3.75 MHz. The tissue Doppler imaging technique [6]–[10]—modified ultrasound two-dimensional (2-D) color flow mapping—enables us to acquire motion distribution of the myocardium. Even in this measurement, however, the sampling frequency of the displayed motion of the heart wall is low (at most 60 Hz). All these previous clinical methodologies, therefore, are employed to measure only large ($>$ 0.4 mm) and slow ($<$ 30 Hz) motion due to the heartbeat which can be recognized by medical doctors with the naked eye.

By artificially actuating shear waves in tissues or phantoms, their propagation speed and/or viscoelasticity can be determined for tissue characterization [11]–[17]. Yet spontaneously actuated vibrations propagating in the heart wall, which differ from electrically excited waves [18], [19], have not been recognized at all.

In this paper, using a newly developed method to measure spatial distribution of the minute vibrations in the heart wall from the chest wall using ultrasound [20], we find that some impulses propagate along the heart wall in healthy human subjects just after closure of the aortic valve for the first time and their propagation speed shows frequency dispersion, which agrees with the theoretical characteristics of the Lamb wave [21], [22].

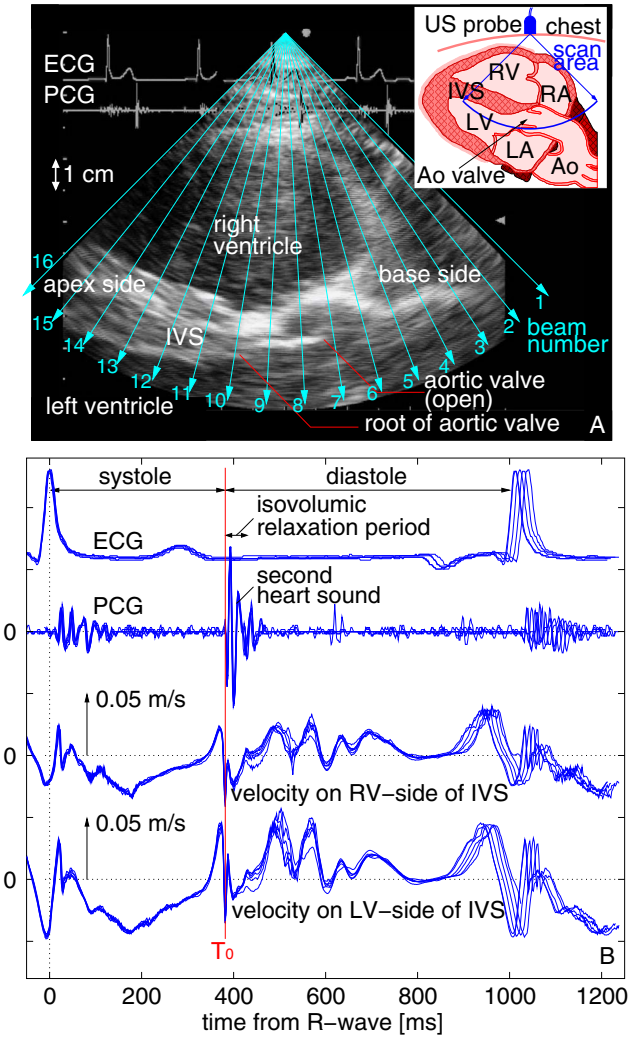

Fig. 1. **(A)** A cross-sectional image measured by a conventional ultrasound diagnosis system for a young healthy male. The upper-right illustration shows the scanning range of the ultrasonic beams in this imaging. **(B)** *In vivo* measurement results for the healthy man in **Fig. A** at two points set along the 13th ultrasonic beam. Each waveform for six consecutive cardiac cycles was overlaid. The timing of the aortic-valve closure is denoted by T_0. (LV: left ventricle, LA: left atrium, RV: right ventricle, RA: right atrium, US probe: ultrasonic probe, IVS: interventricular septum, Ao: aorta, ECG: electrocardiogram, PCG: phonocardiogram (heart sound).)

II. *In Vivo* EXPERIMENTS

Figure 1A shows a typical cross-sectional image of a heart obtained by conventional echocardiography for a young healthy subject from the transthoracic parasternal longitudinal-axis view. The upper-right illustration shows the scanning range of the ultrasonic beams in this imaging. From the motion picture of **Fig. 1A**, the large slow motion during one heartbeat can indeed be recognized.

A. Distribution of the Vibrations in and on the Heart Wall

To measure the original vibrations of the heart sounds audible by stethoscope, we have developed an ultrasound-based transthoracic method to directly measure the heart wall vibrations [23]–[25]. For this measurement, the sampling frequency (the time resolution) should be increased from the 30 Hz in conventional echocardiography to about 500 Hz. To realize this, the number of the transmitted directions of the ultrasonic beams was decreased from 240 to 16 as shown in blue arrows of **Fig. 1A**. For all of the multiple points preset at 75-μm intervals in the heart wall along 16 ultrasonic beams, the vibrations were simultaneously measured as a waveform with a sampling frequency of 450 Hz for the first time by the newly developed phased tracking method [23], [24]. **Figure 1B** shows a typical example of the vibrations on both sides—the right ventricular (RV) side and left ventricular (LV) side—of the interventricular septum (IVS) for the subject in **Fig. 1A**. Though 6 consecutive heartbeats were overlaid, small, rapid vibrations were measured with high reproducibility, although they cannot be observed by any conventional equipment. As shown by these waves, some discriminative impulses can be observed, especially at end-systole. At end-systole, a slow upward pulse continued for about 30 ms before the aortic-valve (AV) closure timing T_0. A steep downward impulse then occurred at T_0 for the beginning of the isovolumic relaxation (IR) period [26].

By applying the same method to about 160 points preset at the AV closure timing T_0 at equal intervals of 770 μm in the IVS along each of the 16 scan lines, the vibration was simultaneously obtained for each point during the short-period between T_0-35 ms to T_0+35 ms. The occurrence of dips was gradually delayed from the root of AV to the apex-side by several milliseconds. To the contrary, a steep upward impulse propagated from the root of AV to the base-side of the heart.

B. Propagation Speed of the Impulse Along the Heart Wall

Since the wavelength of the detected impulsive wave is about 10 cm for a 30 Hz component and is comparable to that of the heart wall, its propagation phenomenon cannot be visualized by showing the amplitude distribution of the resultant impulsive wave along the IVS. Instead, the *phase* value varies from 0 to 360 degrees in one wavelength. In this paper, therefore, 2-D spatial distribution of the instantaneous phase values of the measured wave for a selected frequency component from 10 Hz to 100 Hz is color-coded [20]. **Figure 2** shows this distribution for a 60 Hz frequency component. For this imaging, the short-time Fourier transform was applied to

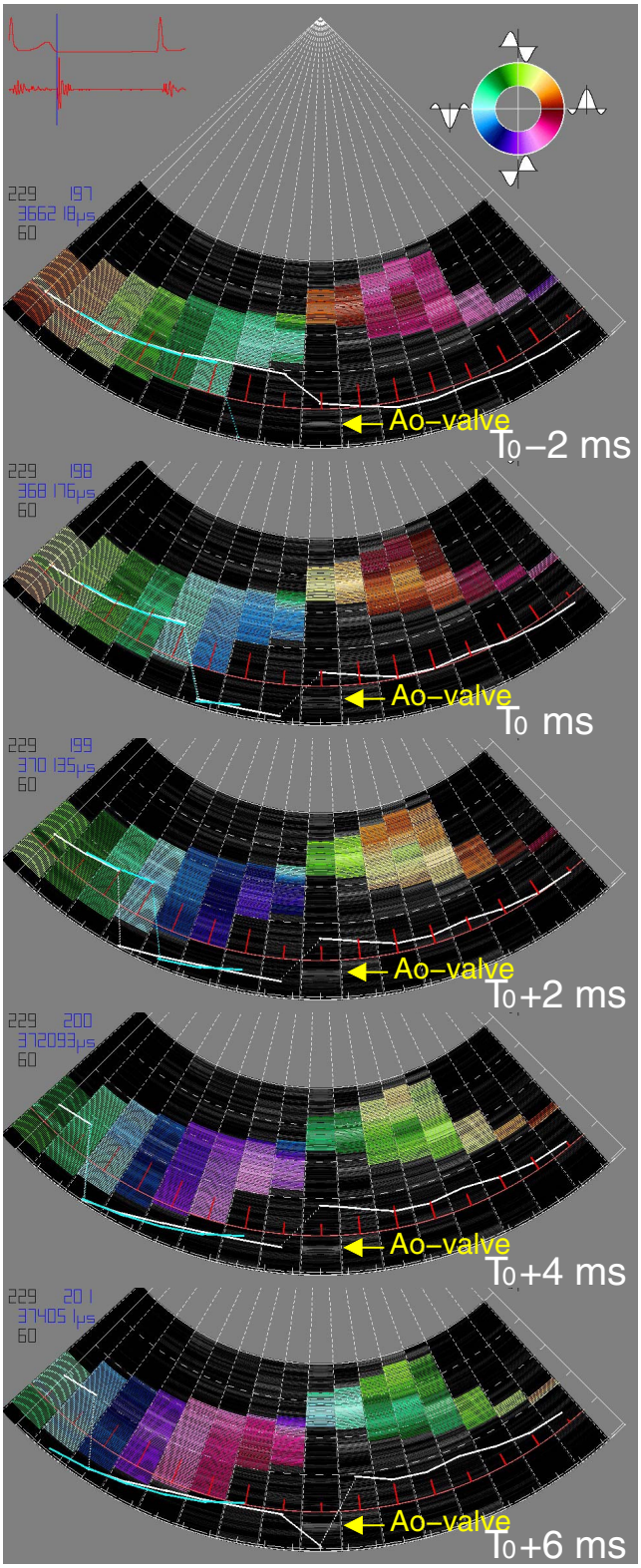

Fig. 2. Spatial distribution of color-coded phase values for 60 Hz component of the measured wavelets at end-systole of the subject in **Fig. 1** consecutively from $T_0 - 2$ ms to $T_0 + 6$ ms around the aortic-valve closure timing T_0. (ECG: electrocardiogram, PCG: phonocardiogram, LV: left ventricle, RV: right ventricle, IVS: interventricular septum, Ao: aorta.)

the wave at each point in the IVS after the wave was multiplied by the Hanning window with a short length of 35 ms. For example, at a time t = T_0-2 ms in **Fig. 2**, the phase values varied from cyan (+180 degrees) near the root of the AV, through green (+90 degrees), to red (0 degree) at the apex-side. This fact shows that for the frequency component (f_0 = 60 Hz) of the downward steep impulse around the timing T_0 in **Fig. 1B**, the time delay gradually increased from 0 ms near the root of the AV to +9 ms (= +180/(360$\times f_0$)) near the apex-side. Moreover, from these consecutively obtained cross-sectional 2-D images in **Fig. 2**, a motion picture can be shown for each frequency component. As shown in the consecutively obtained figures in **Fig. 2** and the motion picture, just around the time of AV closure, a few impulses are radiated from the root of AV and propagated along the IVS. The delay due to the propagation of the steep impulse from the root to the apex-side is several milliseconds, which has not been recognized at all by any other clinical technique.

The instantaneous phase of the impulse at the LV-surface of the IVS spatially varied as an almost straight line from the root to the apex-side as shown by a white line in the left-hand side in each panel of **Fig. 2**. The propagation distance can be measured in the cross-sectional image as in **Fig. 1A**. By fitting the straight line (the cyan line in **Fig. 2**) with a constant gradient k [radian/m] to the spatial distribution of the measured phase, the instantaneous phase velocity v_p [m/s] for the frequency component f_0 was determined by

$$v_p = \frac{2\pi f_0}{k}. \tag{1}$$

Just at the AV closure timing T_0, for example, the instantaneous phase velocities $\{v_p\}$ of the 27, 60, and 87 Hz components of the impulse were, respectively, 2.0, 4.3, and 4.9 m/s, the order of magnitude of which is the same as those measured for human tissues in the literature [11]–[13], [27]. For each timing of each frequency component, by analysing the phase of the wavelets, the instantaneous phase velocity was measured as in **Fig. 3**. From end-systole to the beginning of the IR period, there was dispersion among the instantaneous phase velocities, and they rapidly decreased for all frequency components of 10-100 Hz.

C. Determination of Instantaneous Viscoelasticity

In the parasternal longitudinal-axis view of **Fig. 2**, the direction of each ultrasonic beam is almost perpendicular to the IVS, and the vibration is detected in the direction along each ultrasonic beam. As shown in **Fig. 2**, the propagation direction is almost perpendicular to the direction of the detected vibration. This phenomenon is explained by a Lamb wave—a shear vertical wave of the guided wave [21], [22] in a thin wall (IVS) with a thickness of $2d$. The theoretical phase velocity v_p of the Lamb wave at the frequency f_0 is given by [22]

$$v_p = \sqrt[4]{\frac{4\mu(\lambda+\mu)}{3\rho(\lambda+2\mu)}}\sqrt{2\pi f_0 d}, \tag{2}$$

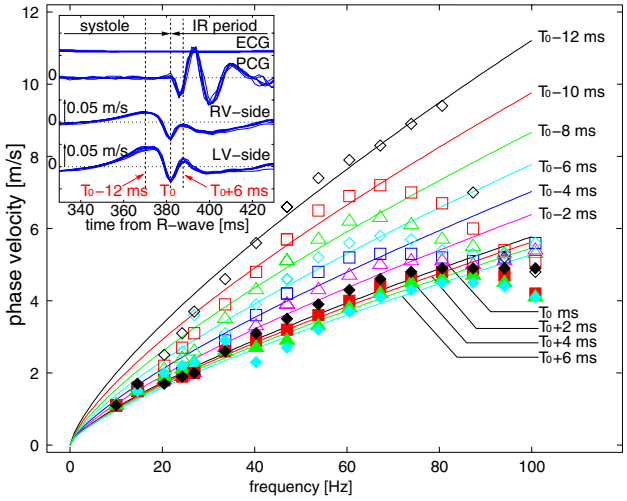

Fig. 3. Measured instantaneous phase velocity values $\{v_p\}$ and fitted theoretical lines of Eq. (3) for frequency components from 10 Hz to 100 Hz during the period from $T_0 - 12$ ms to $T_0 + 6$ ms in **Fig. 1B**. The upper left figure again shows the four waveforms in **Fig. 1B** but after expansion in the time axis from end-systole to the beginning of the isovolumic relaxation (IR) period. (ECG: electrocardiogram, PCG: phonocardiogram, RV: right ventricle, LV: left ventricle)

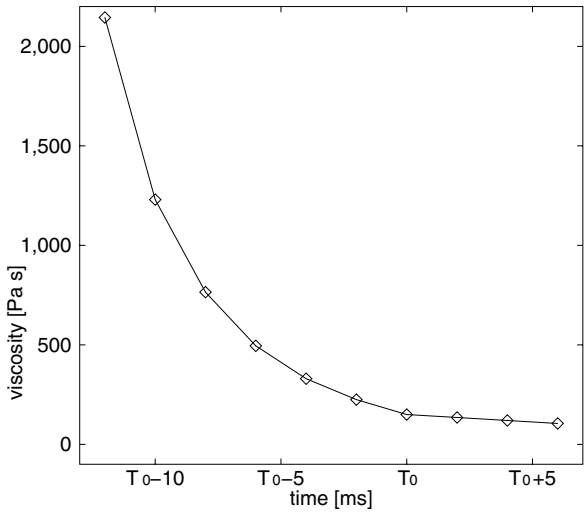

Fig. 4. Transient of the viscosity parameters $\{\mu_2\}$ measured during the period from $T_0 - 12$ ms to $T_0 + 6$ ms in **Fig. 3**.

where ρ is the density of the tissue, μ and λ are the Lamè's constants showing the coefficients of shear viscoelasticity and volume viscoelasticity, respectively. From the experimental results [27], $\lambda \gg \mu$. By assuming a simple Voigt model with one spring and one dash-pot in the measured frequency range up to 100 Hz, the shear viscoelasticity parameter μ is given by a complex value, that is, $\mu = \mu_1 + j2\pi f_0 \mu_2$. Thus, the theoretical value of the phase velocity v_p of Eq. (2) is approximated by

$$v_p = \sqrt[4]{\frac{4}{3\rho}}\Re\left[\sqrt[4]{\mu_1 + j2\pi f_0 \mu_2}\right]\sqrt{2\pi f_0 d}, \tag{3}$$

where $\Re[\cdot]$ denotes the real part, $2d$ is about 10 mm and can be measured in the cross-sectional image of **Fig. 1**, and ρ is assumed to be 1.1×10^3 kg/m^3. By fitting Eq. (3) to the measured instantaneous phase velocities $\{v_p\}$ from 10 to 100 Hz in **Fig. 3**, the instantaneous elasticity parameter μ_1 and viscosity parameter μ_2 were determined. As shown in **Fig. 3**, the phase velocity v_p approached zero for low frequency f_0. Thus, the shear elasticity μ_1 in Eq. (3) was negligibly small. The shear viscosity μ_2 corresponds to the gradient of the dispersion curve. **Figure 4** shows the transient of the viscosity parameters $\{\mu_2\}$ determined for each timing from T_0-12 ms to T_0+6 ms in **Fig. 3**. For end-systole to the beginning of the IR period, the instantaneous viscosity of the myocardium rapidly decreased from about 2.1 kPa·s to 0.1 kPa·s. This would be due to the rapid decrease in the LV inner pressure from about 120 to several mmHg, which is caused by relaxation of the myocardium. These viscosity values have same order of magnitude as those measured for canine hearts [28].

III. Conclusions

To conclude, we measured rapid and minute vibration signals, which differ from electrically excited waves, simultaneously at multiple points in the IVS to image the wavefront propagation along the heart wall. For the IR period, clear propagation of the steep impulses from the root of the AV to the apex-side was recognized for the first time. From the dispersion of their phase velocities, the viscosity parameter was determined noninvasively. This method offers potential for in vivo imaging of the spatial distribution of the regional viscoelasticity in the myocardium and its rapid change during the IR period, which enable direct assessment of diastolic function based on myocardial relaxation for heart failure [29], [30].

References

[1] E. A. Zerhouni, D. M. Parish, W. J. Rogers, A. Yang, and E. P. Shapiro, "Human heart: tagging with MR imaging – a method for noninvasive assessment of myocardial motion," *Radiology*, vol. 169, pp. 59-63, 1988.

[2] L. Axel, R. C. Goncalves, and D. Bloomgarden, "Regional heart wall motion: two-dimensional analysis and functional imaging with MR imaging," *Radiology*, vol. 183, no. 3, pp. 745-750, 1992.

[3] L. T. Mahoney, W. Smith, M. P. Noel, M. Florentine, D. J. Skorton, and S. M. Collins, "Measurement of right ventricular volume using cine computed tomography," *Invest. Radiol.*, vol. 22, no. 6, pp. 451-455, 1987.

[4] A. D. Fleming, X. Xia, W. N. McDicken, G. R. Sutherland, and L. Fenn, "Myocardial velocity gradients detected by Doppler imaging," *Br. J. Radiol.*, vol. 67, no. 799, pp. 679-688, 1994.

[5] R. S. Adler, J. M. Rubin, P. H. Bland, and P. L. Carson, "Quantitative tissue motion analysis of digitized M-mode images: gestational differences in fetal lung," *Ultrasound Med. Biol.*, vol. 16, no. 6, pp. 561-569, 1990.

[6] G. R. Sutherland, C. M. Moran, A. D. Fleming, F. J. Guell-Peris, R. A. Riemersma, L. N. Fenn, K. A. A. Fox, and W. N. McDicken, "Color Doppler myocardial imaging: a new technique for the assessment of myocardial function.," *J. Am. Soc. Echocardiogr.*, vol. 7, pp. 441-458, 1994.

[7] A. Heimdal, A. Støylen, H. T. Drtechn, and T. Skjærpe, "Real-time strain rate imaging of the left ventricle by ultrasound," *J. Am. Soc. Echocardiogr.*, vol. 11, pp. 1013-1019, 1998.

[8] M. Uematsu, K. Miyatake, N. Tanaka, H. Matsuda, A. Sano, N. Yamazaki, and M. Hirama, "Myocardial velocity gradient as a new indicator of regional left ventricular contraction: detection by a two-dimensional tissue Doppler imaging technique," *J. Am. Coll. Cardiol.*, vol. 26, no. 1, pp. 217-223, 1995.

[9] P. Palka, A. Lange, A. D. Fleming, L. N. Fenn, K. P. Bouki, T. R. D. Shaw, K. A. A. Fox, and W. N. McDicken, "Age-related transmural peak mean velocities and peak velocity gradients by Doppler myocardial imaging in normal subjects," *Eur. Heart J.*, vol. 17, pp. 940-950, 1996.

[10] J. Goecsan III, V. K. Gulati, W. A. Mandarino, and W. E. Katz, "Color-coded measures of myocardial velocity throughout the cardiac cycle by tissue Doppler imaging to quantify regional left ventricular function," *Am. Heart J.*, vol. 131, pp. 1203-1213, 1996.

[11] Y. Yamakoshi, J. Sato, and T. Sato, "Ultrasonic imaging of internal vibration of soft tissue under forced vibration," *IEEE Trans. Ultrason., Ferroelect., Freq. Contr.*, vol. 37, no. 2, pp. 45-53, 1990.

[12] S. F. Levinson, M. Shinagawa, and T. Sato, "Sonoelastic determination of human skeletal muscle elasticity," *J. Biomechanics*, vol. 28, pp. 1145-1153, 1995.

[13] S. Catheline, J-L. Thomas, F. Wu, and M. A. Fink, "Diffraction field of a low frequency vibration in soft tissues using transient elastography," *IEEE Trans. Ultrason., Ferroelect., Freq. Contr.*, vol. 105, pp. 2941-2950, 1999.

[14] S. Catheline, F. Wu, and M. Fink, "A solution to diffraction biases in sonoelasticity: The acoustic impulse technique," *J. Acoust. Soc. Am.*, vol. 46, pp. 1013-1019, 1999.

[15] L. Sandrin, M. Tanter, S. Catheline, and M. Fink, "Shear modulus imaging with 2-D transient elastography," *IEEE Trans. Ultrason., Ferroelect., Freq. Contr.*, vol. 49, no. 4, pp. 426-435, 2002.

[16] V. Dutt, R. R. Kinnick, and J. F. Greenleaf, "Acoustic shear wave displacement using ultrasound," *1996 IEEE Ultrason. Sympo. Proc.*, pp. 1185-1188, 1996.

[17] S. Chen, M. Fatemi, and J. F. Greenleaf, "Complex stiffness quantification using ultrasound stimulated vibrometry," *2003 IEEE Ultrason. Sympo. Proc.*, pp. 941-944, 2003.

[18] O. Anosov, S. Berdyshev, I. Khassanov, M. Schaldach, and B. Hensel, "Wave propagation in the atrial myocardium: Dispersion properties in the normal state and before fibrillation," *IEEE Trans. Biomed. Eng.*, vol. 49, no. 12, pp. 1642-1645, 2002.

[19] S. P. Thomas, J. P. Kucera, L. Bircher-Lehmann, Y. Rudy, J. E. Saffits, A. G. Kléber, "Impulse propagation in synthetic strands of neonatal cardiac myocytes with generally reduced levels of connexin43," *Circ. Res.*, vol. 92, pp. 1209-1216, 2003.

[20] H. Kanai, and Y. Koiwa, "Myocardial rapid velocity distribution," *Ultrasound Med. Biol.*, vol. 27, no. 4, pp. 481-498, 2001.

[21] H. F. Tiersten, *Linear Piezoelectric Plate Vibrations* New York: Prenum Press, 1969.

[22] I. A. Viktorov, *Rayleigh and Lamb Waves* New York: Prenum Press, 1967.

[23] H. Kanai, M. Sato, Y. Koiwa, and N. Chubachi, "Transcutaneous measurement and spectrum analysis of heart wall vibrations," *IEEE Trans. Ultrason., Ferroelect., Freq. Contr.*, vol. 43, no. 5, pp. 791-810, 1996.

[24] H. Kanai, H. Hasegawa, N. Chubachi, Y. Koiwa, and M. Tanaka, "Noninvasive evaluation of local myocardial thickening and its color-coded imaging," *IEEE Trans. Ultrason., Ferroelect., Freq. Contr.*, vol. 44, no. 4, pp. 752-768, 1997.

[25] H. Kanai, Y. Koiwa, and J. Zhang, "Real-time measurements of local myocardium motion and arterial wall thickening," *IEEE Trans. Ultrason., Ferroelect., Freq. Contr.*, vol. 46, no. 5, pp. 1229-1241, 1999.

[26] H. Kanai, S. Yonechi, I. Susukida, Y. Koiwa, H. Kamada, and M. Tanaka, "Onset of pulsatile waves in the heart walls at end-systole," *Ultrasonics* vol. 38, no. 1, pp. 405-411, 2000.

[27] H. L. Oestreicher, "Field and impedance of an oscillating sphere in a viscoelastic medium with an application to biophysics," *J. Acoust. Soc. Am.*, vol. 23, no. 6, pp. 707-714, 1951.

[28] G. H. Templeton, and L. R. Nardizzi, "Elastic and viscous stiffness of the canine left ventricle," *J. Appl. Physiol.*, vol. 36, no. 1, pp. 123-127, 1974.

[29] T. J. Fraites Jr., A. Saeki, and D. A. Kass, "Effect of altering filling pattern on diastolic pressure-volume curve," *Circulation*, vol. 96, pp. 4408-4414, 1997

[30] S. R. Solomon, and S. A. Glantz, "Regional ischemia increases sensitivity of left ventricular relaxation to volume in pigs," *Am. J. Physiol.*, vol. 276, pp. H1994-H2005, 1999.